

Extinction Enhancement from a Self-Assembled Quantum Dots Monolayer Using a Simple Thin Films Process

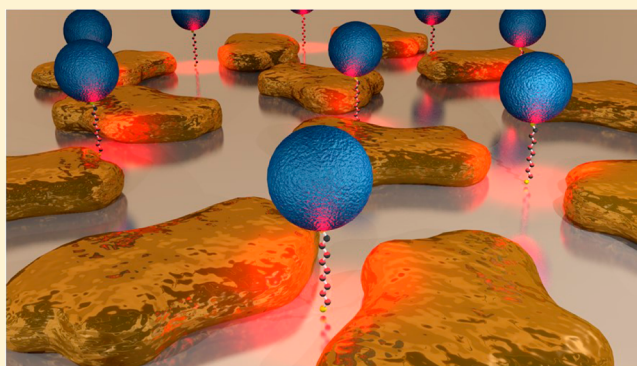
Matan Galanty,[†] Shira Yochelis,[†] Liron Stern,[†] Irene Dujovne,[‡] Uriel Levy,[†] and Yossi Paltiel^{*,†}

[†]Department of Applied Physics, The Hebrew University of Jerusalem, Jerusalem 91904, Israel

[‡]Physics Department, UMass Amherst, Amherst, Massachusetts 01003, United States

S Supporting Information

ABSTRACT: Hybrid nanostructures are attractive for future use in a variety of optoelectronic devices. Self-assembled hybrid organic/quantum dots can couple quantum properties to semiconductor devices and modify their functionality. These devices are simple to fabricate and control; however, they usually demonstrate low quantum efficiency. In this work we present experimental results of large extinction enhancement from a monolayer of colloidal quantum dots using a thin gold film evaporation forming random gold nanoparticles that act as plasmonic antennas. The random structures guarantee no sensitivity to polarization changes. The fabrication process of the plasmonic gold nanoparticles is simple and cheap and can be easily integrated with existing semiconductor devices. By matching the plasmonic resonance and the colloidal quantum dots bandgap we achieve up to 16% light extinction, which is 13-fold enhancement, compared to the reference. These results may pave the way toward realizing more efficient and sensitive photon detectors.



INTRODUCTION

Devices based on self-assembled hybrid colloidal quantum dots (CQDs) and specific organic linker molecules are a promising way to realize room-temperature, spectrally tunable, light detectors. CQDs hold many promising properties such as wavelength, polarization, and lifetime flexibility by the control of material, size, and shape during their growth.¹ Furthermore, CQDs are “substrate free”, making their integration on various platforms simple. They operate at room temperature, even allowing single-photon detection,² and offer the robustness of inorganic materials. These features have led to demonstrations of efficient low-cost photodetectors,^{3,4} light-emitting diodes,⁵ and solar cells.^{6–9}

Despite improvement in electrical properties of CQD films,^{8,10} light absorption from typical films used in solar cells and devices is on the order of 10^4 cm^{-1} , therefore limiting the external quantum efficiency (EQE) of such devices to 30–50% (these films are several hundreds of nanometers thick). Moreover, sensitive devices, down to a single photon level, require highly ordered films, usually by self-assembled methods, which bring down the EQE even more, to the range of a few percent. An essential step to create more sensitive devices is to effectively increase light absorption, at low cost, without sacrificing electronic performance.

Plasmonics has been shown as an efficient tool in guiding and confining light at nanoscale dimensions. The properties of plasmonic resonances are highly sensitive to the size, shape, and composition of the metal and to the local environment

surrounding it.¹¹ This had led to promising applications in many fields such as nanoscale guiding,¹² biosensing and chemical sensing,¹³ metamaterials,¹⁴ and optoelectronic devices.^{15–21}

Moreover, as plasmonic modes exhibit highly confined local fields, they allow us to enhance light–matter interactions and thus can be used to enhance the performance of solar cells,²² light-emitting diodes,²³ and photodetectors.^{24,25}

One typically differentiates between surface plasmon polariton (SPP) modes which can be excited by, e.g., a grating coupler or a prism, and localized surface plasmons (LSPs), which are excited in metal nanostructures and nanoparticles with relative ease.²⁶ Additionally, chemically grown nanostructures may hold excellent plasmonic properties,²⁷ and their production and integration in devices is usually simple and cheap, making them very suitable for enhancing the EQE of solar cells and other devices.

In recent years, several works reported an enhanced photoluminescence (PL) due to enhanced excitation rate.²⁸ Thick CQD films deposited on nanohole arrays,^{29,30} metal nanoparticle arrays,³¹ or gratings³² and circular antenna³³ for directed emission have been demonstrated. CQD film deposited on wrinkled AuPd films³⁴ or on an etched Au/Ag alloy film³⁵ is cheaper and simpler to produce, but it lacks the

Received: August 5, 2015

Revised: October 12, 2015

Published: October 16, 2015

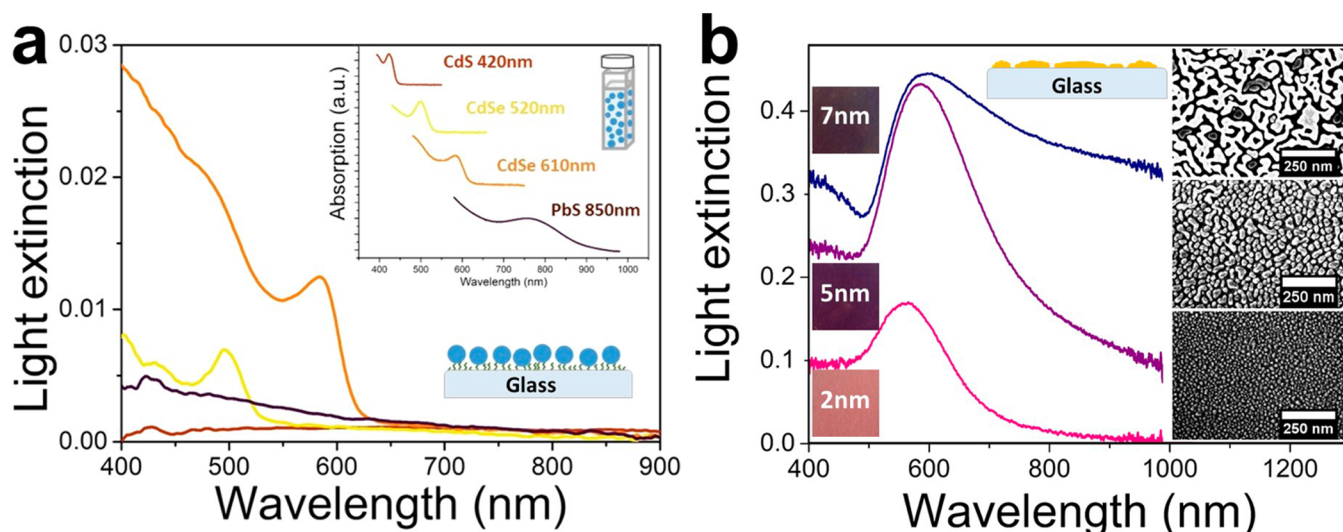


Figure 1. (a) Light extinction from a SAM of CQDs deposited on a glass substrate via organic linkers. In the inset we plot the absorption spectra from a solution of the dots together with a color-coded legend. A schematic illustration of the sample and of the cuvette is added. The thickness of the samples does not exceed several nanometers, and due to this large mismatch in size the small (2.5 nm) particles show only weak scattering, less than 0.005 light extinction. As for the larger particles (5 nm) we note the characteristic absorption spectrum, with 0.01 light extinction at the dot's band gap. (b) Light extinction from the random Au-NP layer deposited on the glass substrate. Left inset shows the color as seen in a microscope. Right inset: SEM images of the random Au-NPs. Bottom image is the 2 nm, middle is 5 nm, and top is 7 nm (nm indicates nominal thickness). The upper inset is a schematic illustration of the sample.

easy integration with semiconductors. An alternative method to create metal nanoparticles is ultrathin metal films that undergo thermal treatment. In this case the surface plasmon resonance can be tuned easily over the visible range.³⁶ This has been used for enhancing absorption in silicon films.³⁷

In this work we experimentally present the coupling properties between random gold nanoparticles (Au-NPs), created by a simple two-stage process, and a self-assembled monolayer (SAM) of CQDs. We use three plasmonic samples of different Au thickness with shifted plasmonic resonance and four types of CQDs with band gap ranging throughout the visible spectrum. We achieve up to 13-fold enhancement in extinction from the CQDs on the plasmonic samples and observe a strong red-shift in the coupled spectrum. The results depend on the detuning between the quantum dot band gap and the plasmonic resonance. This cheap and simple method is suitable for both the nanometric and macroscopic scale and may be easily integrated in various devices for enhancing the EQE.

METHODS

Samples were prepared using two consecutive stages, starting with the plasmonic random structure preparation followed by wet chemistry adsorption of the self-assembled linker molecules and CQDs (see [Supporting Information](#) for detailed procedure).

In the first step glass substrates were cleaned, and a thin Au layer was deposited. The nominal thickness of the films is approximately 2, 5, and 7 nm. To overcome the nonuniform thickness and to adjust the LSPR the samples were annealed on a hot plate for several minutes. These samples are stable for a long period of time and withstand washing and rinsing in water or organic solvents. The average length of the nanoisland was determined manually (see [Supporting Information](#)). For the 2 nm sample the average length is 15 ± 10 nm and for the 5 nm sample 33 ± 15 nm.

In the second step we formed a homogeneous, closely packed single layer of molecules to covalently bind the CQD monolayer onto the plasmonic layer. The samples were first immersed for 17 h in a 1 mM 1,9-nonanedithiol ethanol solution under a nitrogen environment, then washed in absolute ethanol and toluene solutions, and immersed in a diluted 0.05%ww CQD solution for another 17 h and washed in absolute toluene again. We used commercially produced dots with several band gaps: CdS 420 nm, CdSe 520 nm, CdSe 610 nm, and PbS 850 nm (the numbers represent the emission peak wavelengths). Estimating the CQD density on a gold substrate provides a density of $5 \times 10^{11} \text{ cm}^{-2}$.

Only half of the sample was immersed in the solution in order to form a differential sample: the half without the dots was used as a reference in each sample (see schematic sketch in [Figure 2](#) inset).

RESULTS AND DISCUSSION

Plasmonic properties are known to be highly dispersive. As such, spectral analysis is a common tool for surface plasmon characterization. In order to claim a quantitative improvement in extinction we first measure the characteristic light extinction properties of the SAM of CQDs and the random Au-NPs separately and then characterize their coupling. Due to the very small reflection measured from the samples and the reduced scatterings in the optical setup (see [Supporting Information](#)) the light extinction ($1 - \text{transmission}$) indicates mostly the absorption.

[Figure 1\(a\)](#) shows the light extinction from the SAM of CQDs, deposited on glass via organic linkers, used in this work (CdS 420 nm, CdSe 520 nm, CdSe 610 nm, PbS 850 nm—numbers indicate emission wavelength). These samples are taken as a reference and compared to the samples with Au-NPs that enhance the light extinction. The total thickness of the adsorbed linkers and particles does not exceed several nanometers. As a result, the monolayer of the larger particles,

in this experiment the CdSe 610 nm with average size of ~ 5 nm, shows the typical absorption spectrum of CQDs with 0.01 light extinction at the band gap wavelength. The smaller particles, in this experiment the CdS 420 nm and the PbS 850 nm, with average size of ~ 2.5 nm, show only weak scattering, less than 0.005 light extinction. Figure 1(b) displays characteristic light extinction of the random plasmonic layers used in this work, known as localized surface plasmon resonance (LSPR), and scanning electron microscope (SEM) images revealing the random Au-NPs created by the process. SEM images correspond to the extinction graphs of the samples (bottom is 2 nm, top is 7 nm). The inset to Figure 1(b) shows a schematic illustration of the sample (see Supporting Information). As the nominal thickness of the Au film increases, the light extinction increases as well, as expected for a metallic layer. The 2 and 5 nm samples show a very distinct peak, which we attribute to the LSPR of the random Au-NPs, while for the 7 nm the LSPR peak is less obvious. We attribute this difference to the fact that according to the SEM image of the 7 nm sample most of the islands have been connected, forming a more opaque layer. These results are consistent with previous studies done on similar samples³⁷ and on Au nanoparticles in general.^{11,36,38–40}

The plasmonic layer showed no polarization dependency ($<1\%$ change) and may be easily realized on different substrates by using a thin spacer layer.⁴¹ These properties are beneficial for enhancing the EQE of solar cells and other optoelectronic devices based on this method.

In order to investigate the coupling between the random Au-NPs and the SAM of CQDs, we studied different CQDs with bandgaps covering the visible spectrum. Each dot type was chosen to have different coupling strength and resonance detuning relative to the LSPR that remained fixed for all three samples (Au nominal thickness of 2, 5, and 7 nm). Figure 2 shows the characteristic changes in light extinction due to the

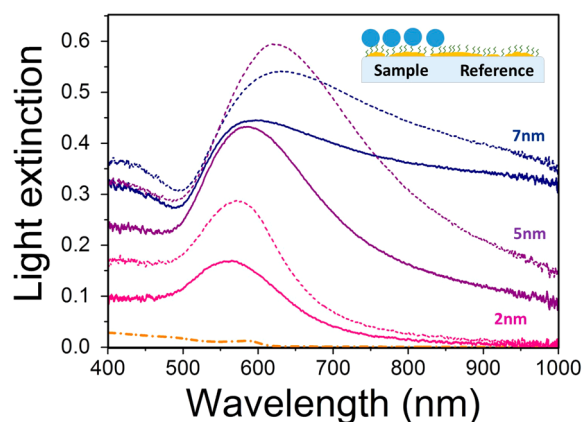


Figure 2. Solid lines: light extinction from the plasmonic nanoisland layer for three different gold layer evaporation thicknesses. The dashed lines: light extinction from the samples with a monolayer of CdSe (610 nm) CQDs adsorbed on the plasmonic layer. The peak absorption of each sample shows an enhancement and a red shift. The orange dashed-dot line shows the light extinction from a monolayer of CQDs on a glass substrate for comparison. The monolayer of CQDs, that contribute 0.01 light extinction when adsorbed on glass, causes 0.1–0.16 light extinction increase when adsorbed on the plasmonic nanoisland layer. The inset displays a schematic sketch of the differential sample (see Supporting Information for the preparation procedure).

adsorption of the dots on top of the random layer. Specifically, this spectrum corresponds to CdSe 610 nm dots. The solid lines correspond to the light extinction from the random Au-NPs from the three different samples, and the dashed lines correspond to the light extinction after the adsorption of the CQD monolayer. The dashed-dotted line at the bottom is the light extinction of the 610 nm dots on glass substrate that serves as a reference. As can be seen in all the samples, the light extinction increase is 0.1 to 0.16 due to coupling for the CQD–Au-NP layer. Compared to the reference on the glass substrate, this increase corresponds to 13-fold enhancement in the light extinction from the samples at the maximum. Furthermore, a clear red-shift is seen for all three samples, although the detuning (energy difference) between the dot's band gap and the plasmonic resonances is the smallest in this specific example.

Figure 3(a) shows the relation between the peak absorption shift and the resonance detuning (energy difference between random Au-NP resonance and CQD bandgap). Figure 3(b) shows the absolute addition of light extinction at the peak absorbance after the CQDs adsorption versus the detuning as well. To extract the data no fitting was done to the plots, and peak absorption was chosen manually.

We observe that both the red shift and the enhancement in extinction increase as the absolute value of the detuning decreases. We interpret these results with the “host medium effect”, as predicted theoretically⁴² and demonstrated experimentally⁴¹ beforehand.

The high refractive index of the inorganic CQDs together with their low absorption coefficient contributes both to the red shift and to the enhanced absorption. The dependence on the detuning indicates the dependence of the real and imaginary parts of the refractive index in the wavelength, which is important in order to maximize the enhancement.

It is interesting to note that the two very detuned dots (CdS 420 nm and PbS 850 nm) showed very weak scattering (less than 0.01 light extinction) when measured on glass substrates as a reference, and on the random Au-NPs layers they contributed up to 0.08 light extinction. Moreover, for the less detuned dots we achieve up to 0.16 light extinction addition, which is a 13-fold enhancement, compared to their reference on a glass substrate.

The errors of the data presented in Figure 3 are estimated to be less than 2%, and the main contribution to the error is the instability of the white light source and the spectrometer. Each measurement was compared to a reference of the same sample, measuring the sample with and without the CQD. The uniformity of the samples (now shown) is very high; therefore, the differential sample produces high quality reference and reduces errors.

For detection applications it is important that the CQD PL was quenched by the metal structures. This is not surprising as the nonanedithiol organic linkers used in this study are approximately 0.6 nm in length, and the quenching of the PL is very strong in that typical length.⁴³ The length of the organic linkers can be easily changed to add another control parameter.

CONCLUSIONS

We have demonstrated tunable enhancement in absorption, up to 13-fold, from a SAM of CQDs using a very accessible and straightforward fabrication method to create a random Au-NP layer. Unlike previous works that showed enhanced absorption or PL, this method uses physically produced random Au-NPs,

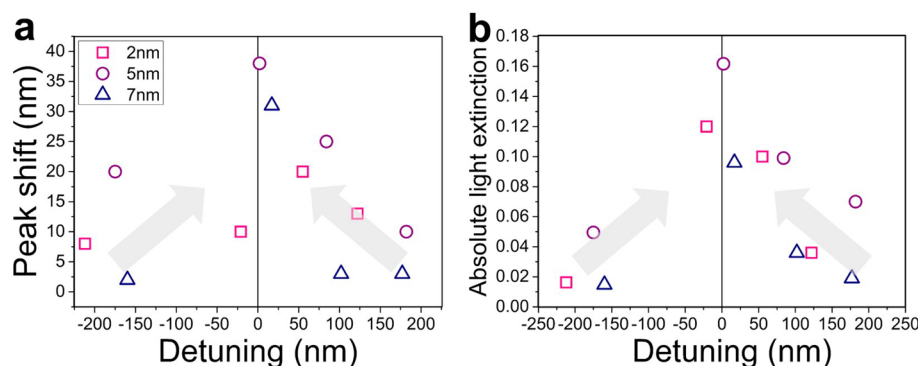


Figure 3. (a) Red-shift increases as the detuning between the CQD band gap and the plasmonic resonance decreases. (b) The absolute light extinction (difference between sample and reference) due to the coupling between the random Au-NP layer and the monolayer of CQDs increases as the detuning decreases. The light gray arrows are used to emphasize the increase in both the red shift and the absolute light extinction, as the detuning decreases. The error of the data is estimated to be smaller than 2%.

which are simple, cost-effective, can be used in a nanoscale or macroscale, and may be easily realized on any substrate. These results may support further improvement in optoelectronic devices.

■ ASSOCIATED CONTENT

● Supporting Information

The Supporting Information is available free of charge on the ACS Publications website at DOI: 10.1021/acs.jpcc.5b07583.

Fabrication procedures, optical characterization details, and additional measurements (PDF)

■ AUTHOR INFORMATION

Corresponding Author

*E-mail: paltiel@mail.huji.ac.il.

Notes

The authors declare no competing financial interest.

■ ACKNOWLEDGMENTS

This research was supported by The Israel's Ministry of Economy grant (Kamin #55260). We would like to thank the Center for Nanoscience and Nanotechnology of the Hebrew University of Jerusalem.

■ REFERENCES

- Alivisatos, A. P. Semiconductor Clusters, Nanocrystals, and Quantum Dots. *Science* **1996**, *271*, 933–937.
- Brokmann, X.; Giacobino, E.; Dahan, M.; Hermier, J. P. Highly Efficient Triggered Emission of Single Photons by Colloidal CdSe/ZnS Nanocrystals. *Appl. Phys. Lett.* **2004**, *85*, 712–714.
- Konstantatos, G.; Sargent, E. H. Nanostructured Materials for Photon Detection. *Nat. Nanotechnol.* **2010**, *5*, 391–400.
- Clifford, J. P.; Konstantatos, G.; Johnston, K. W.; Hoogland, S.; Levina, L.; Sargent, E. H. Fast, Sensitive and Spectrally Tuneable Colloidal-Quantum-Dot Photodetectors. *Nat. Nanotechnol.* **2009**, *4*, 40–44.
- Caruge, J. M.; Halpert, J. E.; Wood, V.; Bulović, V.; Bawendi, M. G. Colloidal Quantum-Dot Light-Emitting Diodes with Metal-Oxide Charge Transport Layers. *Nat. Photonics* **2008**, *2*, 247–250.
- Gur, I.; Fromer, N. A.; Geier, M. L.; Alivisatos, A. P. Air-Stable All-Inorganic Nanocrystal Solar Cells Processed from Solution. *Science* **2005**, *310*, 462–465.
- Sun, B.; Findikoglu, A. T.; Sykora, M.; Werder, D. J.; Klimov, V. I. Hybrid Photovoltaics Based on Semiconductor Nanocrystals and Amorphous Silicon. *Nano Lett.* **2009**, *9*, 1235–1241.
- Tang, J.; Sargent, E. H. Infrared Colloidal Quantum Dots for Photovoltaics: Fundamentals and Recent Progress. *Adv. Mater.* **2011**, *23*, 12–29.
- Debnath, R.; Bakr, O.; Sargent, E. H. Solution-Processed Colloidal Quantum Dot Photovoltaics: A Perspective. *Energy Environ. Sci.* **2011**, *4*, 4870.
- Konstantatos, G.; Sargent, E. H. *Colloidal Quantum Dot Optoelectronics and Photovoltaics*; Cambridge University Press: U.K., 2013.
- Myroshnychenko, V.; Rodríguez-Fernández, J.; Pastoriza-Santos, I.; Funston, A. M.; Novo, C.; Mulvaney, P.; Liz-Marzán, L. M.; Abajo, F. J. G. de. Modelling the Optical Response of Gold Nanoparticles. *Chem. Soc. Rev.* **2008**, *37*, 1792–1805.
- Barnes, W. L.; Dereux, A.; Ebbesen, T. W. Surface Plasmon Subwavelength Optics. *Nature* **2003**, *424*, 824–830.
- Homola, J. Surface Plasmon Resonance Sensors for Detection of Chemical and Biological Species. *Chem. Rev.* **2008**, *108*, 462–493.
- Yao, K.; Liu, Y. Plasmonic Metamaterials. *Nanotechnol. Rev.* **2013**, DOI: 10.1515/ntrev-2012-0071.
- Akbari, A.; Tait, R. N.; Berini, P. Surface Plasmon Waveguide Schottky Detector. *Opt. Express* **2010**, *18*, 8505.
- Berini, P. Surface Plasmon Photodetectors and Their Applications. *Laser Photonics Rev.* **2014**, *8*, 197–220.
- Goykhman, I.; Desiatov, B.; Khurgin, J.; Shappir, J.; Levy, U. Locally Oxidized Silicon Surface-Plasmon Schottky Detector for Telecom Regime. *Nano Lett.* **2011**, *11*, 2219–2224.
- Goykhman, I.; Desiatov, B.; Khurgin, J.; Shappir, J.; Levy, U. Waveguide Based Compact Silicon Schottky Photodetector with Enhanced Responsivity in the Telecom Spectral Band. *Opt. Express* **2012**, *20*, 28594–28602.
- Sobhani, A.; Knight, M. W.; Wang, Y.; Zheng, B.; King, N. S.; Brown, L. V.; Fang, Z.; Nordlander, P.; Halas, N. J. Narrowband Photodetection in the near-Infrared with a Plasmon-Induced Hot Electron Device. *Nat. Commun.* **2013**, *4*, 1643.
- Knight, M. W.; Wang, Y.; Urban, A. S.; Sobhani, A.; Zheng, B. Y.; Nordlander, P.; Halas, N. J. Embedding Plasmonic Nanostructure Diodes Enhances Hot Electron Emission. *Nano Lett.* **2013**, *13*, 1687–1692.
- Zheng, B. Y.; Wang, Y.; Nordlander, P.; Halas, N. J. Color-Selective and CMOS-Compatible Photodetection Based on Aluminum Plasmonics. *Adv. Mater.* **2014**, *26*, 6318–6323.
- Atwater, H. A.; Polman, A. Plasmonics for Improved Photovoltaic Devices. *Nat. Mater.* **2010**, *9*, 205–213.
- Kwon, M.-K.; Kim, J.-Y.; Kim, B.-H.; Park, I.-K.; Cho, C.-Y.; Byeon, C. C.; Park, S.-J. Surface-Plasmon-Enhanced Light-Emitting Diodes. *Adv. Mater.* **2008**, *20*, 1253–1257.
- Plasmonic Enhanced Optoelectronic Devices*; Springer: New York, 2014.

- (25) Sundararajan, S. P.; Grady, N. K.; Mirin, N.; Halas, N. J. Nanoparticle-Induced Enhancement and Suppression of Photocurrent in a Silicon Photodiode. *Nano Lett.* **2008**, *8*, 624–630.
- (26) Pitarke, J. M.; Silkin, V. M.; Chulkov, E. V.; Echenique, P. M. Theory of Surface Plasmons and Surface-Plasmon Polaritons. *Rep. Prog. Phys.* **2007**, *70*, 1–87.
- (27) Shao, L.; Tao, Y.; Ruan, Q.; Wang, J.; Lin, H.-Q. Comparison of the Plasmonic Performances between Lithographically Fabricated and Chemically Grown Gold Nanorods. *Phys. Chem. Chem. Phys.* **2015**, *17*, 10861–10870.
- (28) Ming, T.; Chen, H.; Jiang, R.; Li, Q.; Wang, J. Plasmon-Controlled Fluorescence: Beyond the Intensity Enhancement. *J. Phys. Chem. Lett.* **2012**, *3*, 191–202.
- (29) Song, J.-H.; Atay, T.; Shi, S.; Urabe, H.; Nurmikko, A. V. Large Enhancement of Fluorescence Efficiency from CdSe/ZnS Quantum Dots Induced by Resonant Coupling to Spatially Controlled Surface Plasmons. *Nano Lett.* **2005**, *5*, 1557–1561.
- (30) Brolo, A. G.; Kwok, S. C.; Cooper, M. D.; Moffitt, M. G.; Wang, C.-W.; Gordon, R.; Riordon, J.; Kavanagh, K. L. Surface Plasmon–Quantum Dot Coupling from Arrays of Nanoholes. *J. Phys. Chem. B* **2006**, *110*, 8307–8313.
- (31) Mendes, M. J.; Hernández, E.; López, E.; García-Linares, P.; Ramiro, I.; Artacho, I.; Antolín, E.; Tobías, I.; Martí, A.; Luque, A. Self-Organized Colloidal Quantum Dots and Metal Nanoparticles for Plasmon-Enhanced Intermediate-Band Solar Cells. *Nanotechnology* **2013**, *24*, 345402.
- (32) Livneh, N.; Strauss, A.; Schwarz, I.; Rosenberg, I.; Zimran, A.; Yochelis, S.; Chen, G.; Banin, U.; Paltiel, Y.; Rapaport, R. Highly Directional Emission and Photon Beaming from Nanocrystal Quantum Dots Embedded in Metallic Nanoslit Arrays. *Nano Lett.* **2011**, *11*, 1630–1635.
- (33) Harats, M. G.; Livneh, N.; Zaiats, G.; Yochelis, S.; Paltiel, Y.; Lifshitz, E.; Rapaport, R. Full Spectral and Angular Characterization of Highly Directional Emission from Nanocrystal Quantum Dots Positioned on Circular Plasmonic Lenses. *Nano Lett.* **2014**, *14*, 5766–5771.
- (34) Ferri, C. G. L.; Inman, R. H.; Rich, B.; Gopinathan, A.; Khine, M.; Ghosh, S. Plasmon-Induced Enhancement of Intra-Ensemble FRET in Quantum Dots on Wrinkled Thin Films. *Opt. Mater. Express* **2013**, *3*, 383–389.
- (35) Zhang, L.; Song, Y.; Fujita, T.; Zhang, Y.; Chen, M.; Wang, T.-H. Large Enhancement of Quantum Dot Fluorescence by Highly Scalable Nanoporous Gold. *Adv. Mater.* **2014**, *26*, 1289–1294.
- (36) Sun, H.; Yu, M.; Wang, G.; Sun, X.; Lian, J. Temperature-Dependent Morphology Evolution and Surface Plasmon Absorption of Ultrathin Gold Island Films. *J. Phys. Chem. C* **2012**, *116*, 9000–9008.
- (37) Gaspar, D.; Pimentel, A. C.; Mateus, T.; Leitão, J. P.; Soares, J.; Falcão, B. P.; Araújo, A.; Vicente, A.; Filonovich, S. A.; Águas, H. Influence of the Layer Thickness in Plasmonic Gold Nanoparticles Produced by Thermal Evaporation. *Sci. Rep.* **2013**, DOI: [10.1038/srep01469](https://doi.org/10.1038/srep01469).
- (38) Long, N. N.; Vu, L. V.; Kiem, C. D.; Doanh, S. C.; Nguyet, C. T.; Hang, P. T.; Thien, N. D.; Quynh, L. M. Synthesis and Optical Properties of Colloidal Gold Nanoparticles. *J. Phys. Conf. Ser.* **2009**, *187*, 012026.
- (39) Zhang, X.; Zhang, J.; Wang, H.; Hao, Y.; Zhang, X.; Wang, T.; Wang, Y.; Zhao, R.; Zhang, H.; Yang, B. Thermal-Induced Surface Plasmon Band Shift of Gold Nanoparticle Monolayer: Morphology and Refractive Index Sensitivity. *Nanotechnology* **2010**, *21*, 465702.
- (40) Karakouz, T.; Holder, D.; Goomanovsky, M.; Vaskevich, A.; Rubinstein, I. Morphology and Refractive Index Sensitivity of Gold Island Films. *Chem. Mater.* **2009**, *21*, 5875–5885.
- (41) Niu, J.; Shin, Y. J.; Son, J.; Lee, Y.; Ahn, J.-H.; Yang, H. Shifting of Surface Plasmon Resonance due to Electromagnetic Coupling between Graphene and Au Nanoparticles. *Opt. Express* **2012**, *20*, 19690.
- (42) García de Arquer, F. P.; Beck, F. J.; Konstantatos, G. Absorption Enhancement in Solution Processed Metal-Semiconductor Nanocomposites. *Opt. Express* **2011**, *19*, 21038.
- (43) Anger, P.; Bharadwaj, P.; Novotny, L. Enhancement and Quenching of Single-Molecule Fluorescence. *Phys. Rev. Lett.* **2006**, *96*, 113002.